IL NUOVO CIMENTO Vol. 37 C, N. 1 Gennaio-Febbraio 2014
DOI 10.1393/ncc/i2014-11694-5

Colloquia: IFAE 2013

Searches for the Higgs boson with $H \to WW \to 2\ell 2\nu$ and $H \to ZZ \to 4\ell$ at CMS

E. Di Marco for the CMS Collaboration

California Institute of Technology - 1200 East California Boulevard Pasadena, CA 91125, USA

ricevuto l'1 Ottobre 2013

Summary. — Searches for the standard model Higgs boson using approximatively $5\,\text{fb}^{-1}$ of 7 TeV and $19.6\,\text{fb}^{-1}$ of 8 TeV pp collisions data collected with the CMS detector at LHC in the fully leptonic channels $H \to WW \to 2\ell 2\nu$ and $H \to ZZ \to 4\ell$ have been performed. In the former channel, an excess of events is observed above background, consistent with the expectations from a Higgs boson of mass around 125 GeV with a statistical significance of 4.0σ. In the latter channel, the boson is observed with a local significance of 6.7σ, with the mass 125.8 ± 0.5 (stat.) ± 0.2 (syst.) GeV. In both channels the observed signal strength $\mu = \sigma/\sigma_{\text{SM}}$, relative to the expectation for the standard model Higgs boson, is consistent with one.

PACS 14.80.Bn – Standard-model Higgs bosons.
PACS 11.15.Ex – Spontaneous breaking of gauge symmetries.
PACS 29.20.db – Storage rings and colliders.

1. – Introduction

One of the open questions in the standard model (SM) of particle physics is the origin of the masses of fundamental particles. Within the SM, vector boson masses arise from the spontaneous breaking of electroweak symmetry by the Higgs field [1,2]. The existence of a particle with mass around 125 GeV, consistent with the associated field quantum, the Higgs boson, has been established experimentally in July 2012 [3,4].

In this conference I reported about the search for the Higgs boson in the $H \to WW \to 2\ell 2\nu$ and $H \to ZZ \to 4\ell$ channels, and the measurements of the properties of the new resonance.

2. – Physics objects selection

The search strategy for these channels is based on a signature with isolated leptons (electrons or muons) and, for $H \to WW \to 2\ell 2\nu$ only, large missing transverse momentum, $E_{\text{T}}^{\text{miss}}$, due to the undetected neutrinos. To improve the signal sensitivity and

measure different production modes, the events are separated by jet multiplicity into mutually exclusive categories. The events are selected by triggers which require the presence of one or two high-p_{T} electrons or muons.

Muon and electron candidates required to be isolated to distinguish between leptons from W,Z-boson decays and those from QCD background processes, which are usually in or near jets. For each lepton candidate, the scalar sum of the transverse energy of all particles compatible with originating from the primary vertex is reconstructed in a cone around its direction. Electron candidates are also identified using a multivariate approach, exploiting information from the tracker, the ECAL, and the combination of these two detectors. For both electrons and muons a correction is applied to account for the contribution to the energy in the isolation cone from the pile-up using the measured median energy density in the event. They are required to originate from the primary vertex of the event. Calibrations of the lepton momentum is performed using samples of millions dilepton resonances, Z, J/ψ and Υ.

Jets are reconstructed using the anti-k_{T} clustering algorithm [5] with distance parameter $D = 0.5$. A similar correction as for the lepton isolation is applied to account for the contribution to the jet energy from the pile-up. Jet energy corrections are applied as a function of the jet E_{T} and η. Within the tracker acceptance the jet tracks are required to be compatible with the primary vertex. Events are classified according to the number of selected jets with $E_{\mathrm{T}} > 30\,\mathrm{GeV}$ and $|\eta| < 4.7$.

In the case of $\mathrm{H} \to \mathrm{WW} \to 2\ell 2\nu$ channel, missing transverse momentum is present in signal events due to $\mathrm{W} \to \ell\nu$ decays. For the $\mathrm{WW} \to \ell\nu\ell\nu$ final state with same-flavor leptons, a large background comes from Drell-Yan process, where no real $E_{\mathrm{T}}^{\mathrm{miss}}$ is present. In this case a *projected* $E_{\mathrm{T}}^{\mathrm{miss}}$ variable is employed [6]. It is equal to the component of $E_{\mathrm{T}}^{\mathrm{miss}}$ transverse to the nearest lepton if the difference in azimuth between this lepton and the $E_{\mathrm{T}}^{\mathrm{miss}}$ vector is less than $\pi/2$. If there is no lepton within $\pi/2$ of the direction of $E_{\mathrm{T}}^{\mathrm{miss}}$ in azimuth, $E_{\mathrm{T}}^{\mathrm{miss}}$ is used directly.

3. – The $\mathrm{H} \to \mathrm{WW} \to 2\ell 2\nu$ channel

Two oppositely charged lepton candidates are required, with $p_{\mathrm{T}} > 20\,\mathrm{GeV}$ for the leading lepton ($p_{\mathrm{T}}^{\ell,\mathrm{max}}$) and $p_{\mathrm{T}} > 10\,\mathrm{GeV}$ for the trailing lepton ($p_{\mathrm{T}}^{\ell,\mathrm{min}}$). Only electrons (muons) with $|\eta| < 2.5$ (2.4) are considered in the analysis. Events with *projected* $E_{\mathrm{T}}^{\mathrm{miss}}$ above 20 GeV are selected for the analysis. To suppress the top-quark background, a *top tagging* technique based on soft-muon and b-jet tagging is applied. A minimum dilepton transverse momentum ($p_{\mathrm{T}}^{\ell\ell}$) of 45 GeV is required to reduce the W+jets background. To reduce the background from WZ production, any event that has a third lepton passing the identification and isolation requirements is rejected. The contribution from Wγ production, where the photon is misidentified as an electron, is reduced by about 90% in the dielectron final state by γ conversion rejection requirements. The contribution from Wγ^* is reduced by the veto on the presence of a third lepton and by isolation requirements. The background from low mass resonances is rejected by requiring a dilepton mass ($m_{\ell\ell}$) greater than 12 GeV. The Drell-Yan process produces same-flavor lepton pairs ($\mathrm{e}^+\mathrm{e}^-$ and $\mu^+\mu^-$). In order to suppress this background, a few additional cuts are applied in the same-flavor final states. First, the resonant component of the Drell-Yan production is rejected by requiring a dilepton mass outside a 30 GeV window centered on the Z pole. Then, the remaining off-peak contribution is suppressed, depending on $m_{\mathrm{H}} < (>) 140\,\mathrm{GeV}$, by a selection on a dedicated multivariate discriminant (a selection

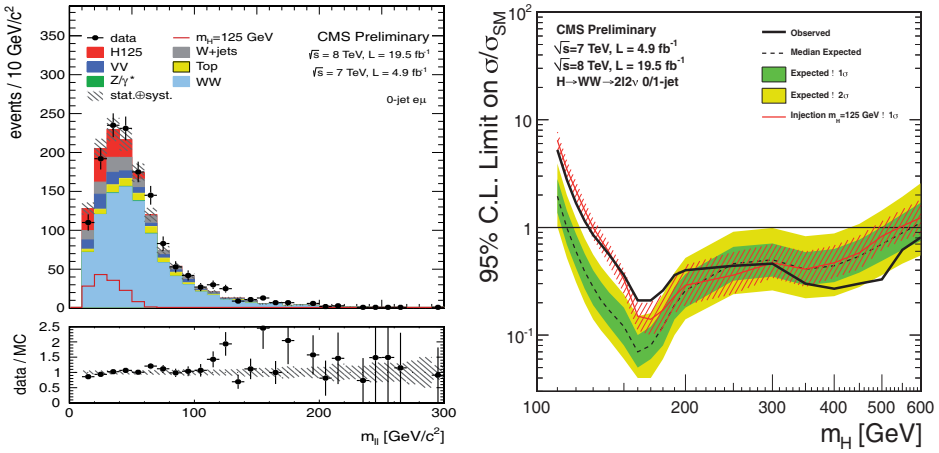

Fig. 1. – Left: distributions of dilepton mass in the 0-jet different-flavor final state for a $m_{\mathrm{H}} = 125\,\mathrm{GeV}$ SM Higgs boson and for the main backgrounds. Right: expected and observed 95% CL upper limits on the cross section times branching fraction, relative to the SM Higgs expectation, using the 7+8 TeV data. The expected limits in the presence of the Higgs with $m_{\mathrm{H}} = 125\,\mathrm{GeV}$ and its associated uncertainty are also shown.

on *projected* $E_{\mathrm{T}}^{\mathrm{miss}} > 45\,\mathrm{GeV}$). This effectively reduce the Drell-Yan background by three orders of magnitude, while rejecting less than 50% of the signal.

A combination of techniques is used to determine the contributions from the background processes that remain after the Higgs selection. Where feasible, background contributions are estimated directly from data. The W+jets and QCD multi-jet backgrounds arise from leptonic decays of heavy quarks, hadrons misidentified as leptons, and electrons from photon conversion. The estimate of these contributions uses a control sample of events in which one lepton passes the standard criteria and the other does not. The normalization of the top-quark background is estimated from data as well by counting the number of top-tagged events and applying the corresponding top-tagging efficiency measured on data with one b-tagged jet. For the low-mass $\mathrm{H} \to \mathrm{WW}$ signal region, $m_{\mathrm{H}} \leq 200\,\mathrm{GeV}$, the non-resonant WW contribution is estimated from data with events with $m_{\ell\ell} > 100\,\mathrm{GeV}$, while for larger m_{H} simulation is used. The $\mathrm{Z}/\gamma^* \to \ell^+\ell^-$ contribution to the $\mathrm{e}^+\mathrm{e}^-$ and $\mu^+\mu^-$ final states is based on extrapolation from the observed number of events with a dilepton mass within $\pm 7.5\,\mathrm{GeV}$ of the Z mass, where the residual background in that region is subtracted using $\ell^+\ell^-$ events. Finally, to estimate the normalization of $\mathrm{W}\gamma^*$ background contribution from asymmetric virtual photon decays, where one lepton escapes detection, a control sample of high purity $\mathrm{W}\gamma^*$ events with three reconstructed leptons is used. Other minor backgrounds from WZ, ZZ (when the two selected leptons come from different bosons) and $\mathrm{W}\gamma$ are estimated from simulation.

After the selection, the number of events counted in data in the different-flavor channels are 1349 (733) and in the same flavor channels are 530 (327) with zero (one) associated jets. In the most sensitive different flavor channels a two-dimensional binned fit based on $m_{\ell\ell} - M_{\mathrm{T}}$ variables is performed, while for the same-flavor channels a cut and count analysis is done, with tighter selections on kinematic variables optimized for each M_{H}. Figure 1 (left) shows the data distribution of the most sensitive variable,

$m_{\ell\ell}$, compared to the simulation, and the results in terms of 95% observed and median expected C.L. upper limits on the ratio of the production cross section to the SM expectation. They are obtained by combining the cut-based analysis in the same-flavor final states and fit-based analysis in the different-flavor final states. The combination of the results from the 7 TeV and 8 TeV data, using the fit-based analysis, excludes a Higgs boson in the mass range 128–600 GeV at 95% CL. The expected exclusion range for the background only hypothesis is 115–575 GeV. An excess of events is observed for hypothetical low Higgs boson masses, which makes the observed limits weaker than the expected ones. This is shown in fig. 1 (right). The observed (expected) significance for $M_{\mathrm{H}} = 125\,\mathrm{GeV}$ is 4.0 (5.0)σ, and best fit value of $\sigma/\sigma_{SM} = 0.76 \pm 0.13\ (\mathrm{stat.}) \pm 0.16\ (\mathrm{syst.}) = 0.76 \pm 0.21$ (stat.+syst.).

4. – The $\mathrm{H} \to \mathrm{ZZ} \to 4\ell$ channel

The $\mathrm{H} \to \mathrm{ZZ} \to 4\ell$ channel is the cleanest channel and it is often referred as the "golden channel". The signal consists of four isolated leptons. For high mass both pairs of opposite charge and same flavour leptons are consistent with Z decays while for lower masses at least one of the pairs has lower mass. The Higgs branching ratio for this channel is rather small, approximately one per mille at high mass and lower for masses below $2 \times m_{\mathrm{W}}$ but the background is very small. The mass resolution is very good and ranges between 1 and 2%. The p_{T} of the lower p_{T} leptons is rather small and one of the most important features of the analysis is the achievement of a very high lepton efficiency down to very low p_{T}. The analysis is carried out in the mass range [110–1000] GeV.

The backgrounds consist of an irreducible component, from continuum ZZ production, which is estimated from simulation, and a reducible background, referred as Z + X, from $\mathrm{Z}\bar{\mathrm{b}}\bar{\mathrm{b}}$, $\mathrm{t}\bar{\mathrm{t}}$, Z + light jets, WZ + jets processes, where at least one of the leptons is misidentified, which is estimated from data control samples. After the selection a good agreement is observed with the SM backgound in the $m_{4\ell} > 160\,\mathrm{GeV}$ range, with the exception of an excess of events, concentrated around 125 GeV (fig. 2). To enhance the sensitivity to the signal, and also to study the properties of the observed resonance, a matrix element likelihood approach is used to construct a kinematic discriminant (K_D) based on the probability ratio of the signal and background hypotheses, $K_D = \mathcal{P}_{\mathrm{sig}}/(\mathcal{P}_{\mathrm{sig}} + \mathcal{P}_{\mathrm{bkg}})$, where the leading-order matrix elements define the probabilities for each value of $m_{4\ell}$ [3]. This information is added to the $m_{4\ell}$ in the likelihood used to extract the signal. To achieve sensitivity to different production modes (gluon fusion or VBF) the events are categorized according to the presence of two jets. In this case a Fisher discriminant is calculated using the jets kinematics, while the Higgs boson candidate $p_{\mathrm{T}}/m_{4\ell}$ is used for the rest of the events. Figure 2 (right) shows the local p-values, as a function of M_{H}, for the low mass range: the minimum is reached around 125.8 GeV, and corresponds to a local significance of 6.7σ (for an expectation of 7.2σ). The signal strength μ, relative to the expectation for the SM Higgs boson, is $\mu = 0.91^{+0.30}_{-0.24}$ at 125.8 GeV.

The mass measurement of the new resonance is performed with a three-dimensional fit using for each event the $m_{4\ell}$, the associated per-event mass error, and the K_D. The resulting fit gives $m_{\mathrm{H}} = 125.8 \pm 0.5\ (\mathrm{stat.}) \pm 0.2\ (\mathrm{syst.})\,\mathrm{GeV}$. The systematic uncertainty accounts for the effect on the mass scale of the lepton momentum scale and resolution.

To disentangle the production mechanisms of the new state (fermion induced or vector boson induced), two signal strength modifiers (μ_F, μ_V) are introduced as scale factors to the SM expected cross section. A two-dimensional fit is performed for the two signal strength modifiers assuming a mass hypothesis of $m_H = 125.8\,\mathrm{GeV}$. The ($\mu_V, \mu_F$) fit

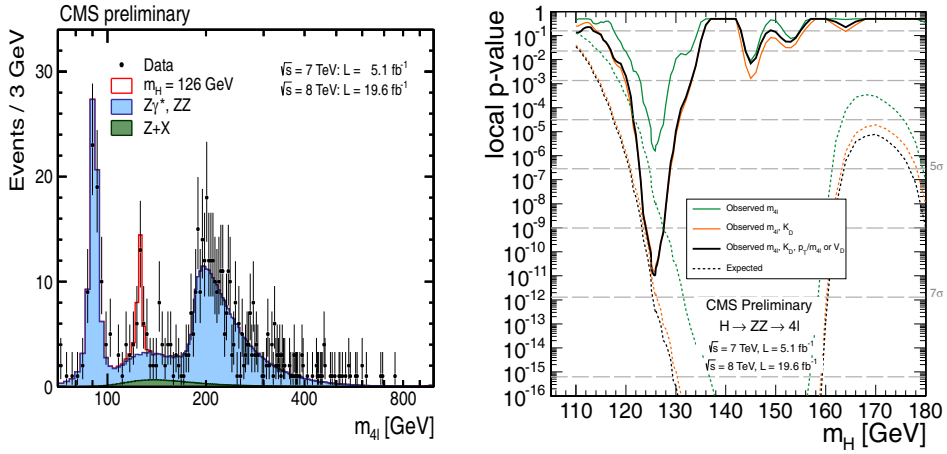

Fig. 2. – Left: distribution of the four-lepton reconstructed mass in the full mass range for the sum of the three 4ℓ channels. Points represent the data, shaded histograms represent the background and the unshaded histogram the signal expectation. Right: significance of the local excess with respect to the SM background expectation as a function of the Higgs boson mass (for $M_{\mathrm{H}} < 180\,\mathrm{GeV}$) for the 1D ($m_{4\ell}$), 2D ($m_{4\ell}$, K_D) and 3D ($m_{4\ell}$, K_D, $p_T/m_{4\ell}$ or V_D) models.

leads to the measurements $\mu_V = 1.0^{+2.4}_{-2.3}$ and $\mu_F = 0.9^{+0.5}_{-0.4}$ The measured values are consistent with the expectations from the production of a SM Higgs boson.

The spin and parity of the new state is also tested by constructing discriminants using the probability ratio for two signal hypotheses (SM and alternative). Six alternative models: $J^P = 0^+, 0^+_h, 0^-, 2^+_{mgg}, 2^+_{mq\bar{q}}, 1^-, 1^+$ are considered. The distribution of $q = -2\ln(\mathcal{L}_{J^P}/\mathcal{L}_{\mathrm{SM}})$ is examined with generated samples of background and signal of seven types (SM 0^+ and six J^P) for $m_H = 126\,\mathrm{GeV}$. The data disfavours the alternative hypotheses J^P with a $\mathrm{CL_s}$ value in the range 0.1–10%. The measurement of the fraction of a *CP*-violating contribution to the decay amplitude expressed through the fraction of the corresponding decay rate is $f_{a3} = 0.00^{+0.23}_{-0.00}$ or equivalently $f_{a3} < 0.58$ at 95% CL.

5. – Conclusions

I have presented the results of the searches for the SM Higgs boson in the $\mathrm{H} \to \mathrm{WW} \to 2\ell 2\nu$ and $\mathrm{H} \to \mathrm{ZZ} \to 4\ell$ channels. The two channels both observe a new state, with a cross section compatible with the SM Higgs boson. The mass is measured with high precision in the four-lepton final state: $m_{\mathrm{H}} = 125.8 \pm 0.5\,(\mathrm{stat.}) \pm 0.2\,(\mathrm{syst.})\,\mathrm{GeV}$. The spin and parity of the new state are compatible with a SM Higgs boson.

REFERENCES

[1] Englert F. and Brout R., *Phys. Rev. Lett.*, **13** (1964) 321.
[2] Higgs P. W., *Phys. Rev. Lett.*, **13** (1964) 508.
[3] Chatrchyan S. *et al.*, *Phys. Lett. B*, **716** (2012) 30.
[4] Aad G. *et al.*, *Phys. Lett. B*, **716** (2012) 1.
[5] Cacciari M., Salam G. P. and Soyez G., *JHEP*, **0804** (2008) 063.
[6] Chatrchyan S. *et al.*, *Phys. Lett. B*, **710** (2012) 91.